ORIGINAL ARTICLE

Enhancement of intratumoral cyclophosphamide pharmacokinetics and antitumor activity in a *P*450 2B11-based cancer gene therapy model

C-S Chen[1], Y Jounaidi[1], T Su and DJ Waxman

Division of Cell and Molecular Biology, Department of Biology, Boston University, Boston, MA, USA

The therapeutic utility of cytochrome *P*450-based enzyme prodrug therapy is well established by preclinical studies and in initial clinical trials. The underlying premise of this gene therapy is that intratumoral *P*450 expression leads to *in situ* activation of anticancer *P*450 prodrugs, such as cyclophosphamide (CPA), with intratumoral accumulation of its activated 4-OH metabolite. In mice bearing 9L gliosarcomas expressing the CPA 4-hydroxylase *P*450 2B6, enhanced tumor apoptosis was observed 48 h after CPA treatment; however, intratumoral 4-OH-CPA levels were indistinguishable from those of *P*450-deficient tumors, indicating that the bulk of activated CPA is derived from hepatic metabolism. In contrast, in 9L tumors expressing *P*450 2B11, a low K_m CPA 4-hydroxylase, intratumoral 4-OH-CPA levels were higher than in blood, liver and *P*450-deficient tumors. Intratumoral 4-OH-CPA increased dose-dependently, without saturation at 140 mg kg^{-1} CPA, suggesting restricted tumor cell permeation of the parent drug. To circumvent this problem, CPA was administered by direct intratumoral injection, which increased the maximum concentration and area under the curve of drug concentration × time (AUC) of intratumoral 4-OH-CPA by 1.8- and 2.7-fold, respectively. An overall 3.9-fold increase in intratumoral 4-OH-CPA AUC, and in antitumor activity, was obtained when CPA release to systemic circulation was delayed using the slow-release polymer poloxamer 407 as vehicle for intratumoral CPA delivery. These findings highlight the advantage of gene therapy strategies that combine low K_m *P*450 prodrug activation enzymes with slow, localized release of *P*450 prodrug substrates.
Cancer Gene Therapy advance online publication, 14 September 2007; doi:10.1038/sj.cgt.7701092

Keywords: *P*450 gene therapy; *P*450 2B11; cyclophosphamide pharmacokinetics; poloxamer 407

Introduction

The chemosensitization of tumor cells by intratumoral (i.t.) activation of anticancer prodrugs is an emerging adjuvant therapy that can increase the efficacy of several commonly used anticancer agents. Intratumoral prodrug activation may be enhanced by introduction of prodrug-activation enzymes of bacterial, viral or mammalian origin using a variety of gene therapy vectors, including retroviruses, adenoviruses, herpes viruses, as well as nonviral vectors.[1–3] Chemosensitization is achieved when an anticancer prodrug is activated locally in tumor cells, which augments cytotoxic responses, both in the prodrug-activating tumor cell and in naive bystander tumor cells exposed to diffusible cytotoxic metabolites.

One such prodrug activation therapy utilizes genes that encode mammalian cytochrome *P*450 enzymes.[4,5] Drug metabolizing *P*450 enzymes are highly expressed in the liver and are generally found at very low levels in human tumors.[6,7] These enzymes catalyze the metabolism of more than 35 anticancer drugs,[8,9] of which 12 drugs, including the widely used alkylating agent prodrug cyclophosphamide (CPA) and its isomer ifosfamide (IFA), are activated via *P*450 metabolism.[10] CPA is used in both adjuvant and high-dose chemotherapy settings and is effective against a broad range of tumors, including breast cancer and lymphomas.[11] Two hepatic cytochromes *P*450, *P*450 2B6 and *P*450 3A4, catalyze a substantial fraction of CPA activation in human liver with electron input from NADPH *P*450 reductase.[12] CPA is converted to 4-OH-CPA, a cell cycle-independent alkylating metabolite that readily diffuses out of hepatocytes and can exert cytotoxicity at distant sites, including tumor and sensitive host tissues. This intrinsic diffusibility of 4-OH-CPA underlies the bystander cytotoxic response that is obtained when CPA is combined with *P*450-prodrug gene therapy.[13] The efficacy of *P*450 gene therapy can be enhanced in several ways, including combination with bioreductive prodrugs that are activated by *P*450 and/or *P*450 reductase,[14,15] by using a metronomic, antiangiogenic CPA treatment schedule,[16,17] and by using tumor cell-replicating herpes virus[18] and adenovirus[19] to spread the therapeutic *P*450 gene and augment tumor cell lysis.

2

In the present study we investigated the activation of CPA *in vivo* in solid tumors that express *P*450 in an effort to improve the pharmacokinetics of CPA metabolism and enhance the efficacy of this *P*450 prodrug-activation strategy. Our findings demonstrate that despite an increase in chemosensitivity, tumor cell expression of the high K_m CPA 4-hydroxylase enzymes *P*450 2B6 and *P*450 2B1, used in recent clinical trials,[20,21] does not lead to a measurable increase in i.t. 4-OH-CPA levels. In contrast, introduction of *P*450 2B11, a low K_m CPA 4-hydroxylase,[22] increases the i.t. concentration of 4-OH-CPA above that found in *P*450-deficient tumors. Further improvements in i.t. pharmacokinetics and increased net tumor cell exposure to 4-OH-CPA were obtained by direct i.t. CPA delivery via a slow-release polymer, substantially enhancing the overall antitumor response.

Materials and methods

Materials
CPA, chloroquine and puromycin were purchased from Sigma-Aldrich (St Louis, MO). 4-hydroperoxy-CPA was obtained from ASTA Pharma (Bielefield, Germany). IFA was obtained from the Drug Synthesis and Chemistry Branch of the National Cancer Institute (Bethesda, MD). Fetal bovine serum (FBS) and Delbecco's modified Eagle's medium (DMEM) were purchased from Life Technologies (Grand Island, NY). F127, a 12 600 average molecular weight ethylene oxide and propylene oxide block copolymer[23] (also known as Pluronic F127, poloxamer 407 and Pluracare F-127 Prill Surfactant), was obtained from BASF Corporation (Florham Park, NJ) and contained 100 p.p.m. BHT. Rat 9L gliosarcoma cells were grown in a humidified, 5% CO_2 atmosphere at 37 °C in DMEM containing 10% FBS, 100 units ml^{-1} penicillin and 100 μg ml^{-1} streptomycin. Casputin (catalog no. SE760) and the caspase 3 substrate Ac-DEVD-AMC (catalog no. P-411) were purchased from Biomol International LP (Plymouth Meeting, PA).

9L tumors expressing P450 and pharmacokinetic studies
9L gliosarcoma cells were infected with pBabe-based retrovirus expressing *P*450 2B1, *P*450 2B6 or *P*450 2B11 cDNA linked to *P*450 reductase cDNA via an internal ribosome entry site sequence (9L/2B1, 9L/2B6 and 9L/2B11 cells, respectively) as described.[24] 9L cells infected with an empty pBabe-based retrovirus were used as *P*450-deficient controls. Immunochemical analysis using anti-*P*450 2B antibodies revealed *P*450 2B expression in ~90–95% of the cultured 9L/2B cells. This percentage decreased to ~50% or less of the cells when grown subcutaneously as solid tumors (J Ma and DJ Waxman, unpublished observations). 9L tumor cells were grown to near-confluence in DMEM culture medium containing 10% FBS, harvested by trypsin digestion, washed once, and resuspended in FBS-free DMEM and placed on ice. Five-week-old (23–25 g) male ICR/Fox Chase outbred immunodeficient scid mice (Taconic Farms, Germantown, NY) were injected subcutaneously on each flank

with 4×10^6 9L, 9L/2B1, 9L/2B6 or 9L/2B11 cells in 0.2 ml of FBS-free DMEM using an 0.3 ml U-100 insulin syringe and a 28G-1/2 needle. All mice were housed and treated in the Boston University Laboratory of Animal Care Facility using approved animal protocols.

Pharmacokinetic data were collected when the tumors reached 800–1000 mm^3 in size. Mice were given a single injection of CPA or IFA at doses specified in each experiment, either by intraperitoneal (i.p.) injection or by direct i.t. injection as described below. In some cases, CPA was dissolved in 0.2% NaCl or in a 23% solution of F127 dissolved in 0.2% NaCl and then injected i.t. as specified in each experiment. The final CPA concentration was adjusted to 12.5–14 mg ml^{-1} based on each individual mouse's body weight (BW) to keep the injected volume (60 μl per tumor) and the CPA dose (50 mg kg^{-1} BW) constant. Intratumoral CPA delivery was achieved using a syringe pump (model KDS100; KD Scientific, Holliston, MA) set a 1 μl s^{-1} with a 30-gauge needle (20 μl per injection × 3 injection sites per tumor). A 23% F127 polymer solution was prepared as follows: 3 g of F127 was dissolved in 7.0 ml of sterile 0.2% NaCl with shaking at 4 °C over a 24-h period to obtain a 30% F127 solution. A sterile solution of 60 mg ml^{-1} CPA was sonicated before use and then mixed with the required volume of 30% F127 stock solution to achieve a final concentration of 23% F127. Thus, for a 30 g mouse to be treated with 1.5 mg CPA (i.e., 50 mg CPA kg^{-1} BW), 208 μl of 60 mg ml^{-1} of CPA solution was mixed with 767 μl of 30% F127 and 25 μl of 0.2% NaCl. A volume of 60 μl was then injected directly into each tumor. Mice were killed 6, 15, 30, 60, 120 and 240 min after CPA treatment ($n = 3$ mice per time point).

4-OH-CPA levels were assayed in 200–400 μl of blood collected by heart puncture using a syringe containing 10 μl of heparin at 100 U ml^{-1} and 2–4 μl of 0.5 M semicarbazide (final concentration 5 mM) to stabilize the 4-OH-CPA. The concentration of 4-OH-CPA in liver and in tumor was determined using ~0.4 g of tissue prewashed with 0.1 M KPi buffer, pH 7.4 containing 0.1 mM EDTA and 5 mM semicarbazide. Tissues were homogenized using a Polytron homogenizer, model PT-2000 (Kinematica, Luzern, Switzerland), in 0.1 M KPi buffer containing 0.1 mM EDTA and 5 mM semicarbazide (5 ml per gram tissue). Homogenized blood, liver and tumor samples were centrifuged in Sorvall SA-600 rotor at 3000 r.p.m. for 30 min at 4 °C, and supernatants were stored at −80 °C prior to high-performance liquid chromatography analysis.

Tumor caspase activity assay
Extracts were prepared from 9L and 9L/2B6 tumors (880 ± 100 mm^3) 24 or 48 h after CPA treatment and then assayed for caspase 3 activity using the fluorogenic caspase 3 substrate Ac-DEVD-AMC as described.[25] Briefly, 0.5 g of tumor tissue was homogenized in 2 ml of lysis buffer (10 mM HEPES, pH 7.4, containing 2 mM EDTA, 0.1% CHAPS, 5 mM DTT, 2 mM PMSF, 10 μg ml^{-1} pepstatin, 10 μg ml^{-1} aprotinin and 20 μg ml^{-1} leupeptin) and then centrifuged at 14 000 r.p.m. for 20 min

in a bench top Eppendorf centrifuge. The supernatant was centrifuged at 35 000 r.p.m. for 1.5 h in a Sorvall T1270 rotor.[26] The resulting supernatant (20 μg protein at 1 mg ml^{-1}) was incubated for 1 h at 37 °C with 500 μl of 50 μM Ac-DEVD-AMC in 10 mM HEPES, pH 7.4, containing 2 mM EDTA, 0.1% CHAPS and 5 mM DTT. The caspase 3 component of this activity was determined in a parallel set of assays carried out after the supernatant fraction was preincubated for 15 min at room temperature with 5 μl of the caspase 3 inhibitor Casputin. Fluorescence was measured (excitation 380 nm, emission 460 nm) using a Shimadzu model RF-1501 spectrofluorophotometer.

Quantification of 4-OH-CPA

4-OH-CPA levels in blood, liver and tumor were determined as described previously.[22] Liver and tumor homogenates were prepared as described above. Blood samples (50 μl) were diluted to 500 μl with 0.1 M KPi buffer, pH 7.4, containing 0.1 mM EDTA and 5 mM semicarbazide. Blood and tissue samples (500 μl) were deproteinized by the sequential addition of 250 μl of 5.5% zinc sulfate and 250 μl of saturated barium hydroxide. Acrolein formed during from the chemical decomposition of 4-OH-CPA was derivatized to 7-hydroxyquinoline and analyzed by high-performance liquid chromatography. A standard curve was generated from 4-hydroperoxy-CPA (0–40 μM) dissolved in KPi buffer and processed in parallel (limit of detection (twice background), 0.3 nmol g^{-1} tissue). Integrated peak areas determined by Millennium[32] software (Waters Corpn, Milford, MA) were then converted into units of nanomole 4-OH-CPA produced per gram tissue.

Pharmacokinetics data analysis

A simple noncompartmental model was used to calculate values for area under the curve (AUCINF$_{observed}$), $t_{1/2}$, maximum concentration (C_{max}) and T_{max} for 4-OH-CPA in blood, liver and tumor using WinNonLin software version 1.5 (Scientific Consulting Inc., Apex, NC). 4-OH-CPA levels in tissue samples derived from CPA-treated mice were corrected for background activity (that is, endogenous acrolein levels) based on the activity measured in the corresponding tissue samples obtained from untreated mice. To calculate pharmacokinetic parameters, the time course data for each tissue was randomly assigned into three separate datasets, each comprised of a full set of data points obtained for one of the three mice killed at each time point. The Descriptive Statistics module of WinNonLin software was used to calculate values for AUCINF$_{observed}$, $t_{1/2}$, C_{max} and T_{max} on the final parameters table in the form of mean values ± s.e.m. Statistical comparisons using a nonparametric *t*-test were performed using Prism software version 4 (GraphPad Software, San Diego, CA).

Tumor growth delay studies

9L/2B11 cells were grown and implanted subcutaneously in ICR/Fox male scid mice as described above. Tumors were grown to a size of ∼500 mm^3, at which time the mice were given two CPA injections at 150 mg kg^{-1} BW spaced 24 h apart. Mice were divided into three groups ($n = 5$ mice and $n = 10$ tumors per group). One group of mice was administered with CPA i.p. (25 mg ml^{-1} CPA stock in 0.2% NaCl; systemic delivery). The other groups of mice were injected with CPA, i.t., in a 23% solution of F127 prepared in 0.2% NaCl, using a syringe pump with 30-gauge needle at 1 μl s^{-1} as described above. Cyclophosphamide was dissolved in the 23% F127/0.2% NaCl vehicle at concentrations ranging from 18.7 to 21.4 mg CPA ml^{-1} based on the weight of each mouse to insure an equal dose of CPA and an equal dose of F127 polymer per mouse. Thus, for a 30 g mouse, a dose of 150 mg CPA kg^{-1} BW (i.e., 4.5 mg CPA 30^{-1} g mouse) was achieved by dissolving 20 mg of CPA · H$_2$O in 1 ml of 23% F127/0.2% NaCl solution, whereas for a 32 g mouse, 21.4 mg of CPA · H$_2$O was dissolved in 1 ml of 23% F127/0.2% NaCl solution. In both cases, a total of 240 μl of the CPA/F127/NaCl solution was injected i.t. (6 × 20 μl injected into each tumor). Control mice were injected with 240 μl of 0.2% NaCl. Tumor sizes (length L and width W) were measured twice a week using an electronic digital caliper (VWR international, Marlboro, MA). A second CPA treatment cycle was administered when the tumors reached a size of ∼800 mm^3, that is, day 35 after the first CPA treatment. Tumor volumes were calculated using the formula: volume = π/6 (L × W)$^{3/2}$. Percent tumor regression was calculated as $100 \times (V_1 - V_2)/V_1$, where V_1 is the tumor volume on the day of drug treatment and V_2 is the volume corresponding to the maximum observed decrease in tumor size following drug treatment. Tumor doubling time was calculated as the period of time required for tumors to double in volume after the second drug treatment.[27]

Results

CPA-induced apoptosis in 9L/2B6 tumors

Scid mice bearing 9L/2B6 or *P*450-deficient 9L control tumors were treated with CPA and killed 24 or 48 h later. Tumor homogenates were prepared and assayed for the activity of caspase 3, an effector caspase that is activated in CPA-treated 9L tumor cells.[25] CPA induced a significantly greater increase in caspase 3 activity in the *P*450 2B6-expressing tumors than in the *P*450-deficient tumors (Figure 1). This differential response can be attributed to the activation of CPA locally, within the 9L/2B6 tumor cells, and is consistent with the much stronger antitumor effect seen upon CPA treatment of 9L/2B6 tumors compared to 9L tumors.[17,28]

4-OH-CPA levels in 9L/2B6 and 9L/2B1 tumors

Next we investigated whether the *P*450-dependent increase in CPA-induced apoptosis seen in 9L/2B6 tumors is associated with increased i.t. exposure to 4-OH-CPA, the active metabolite of CPA. Scid mice bearing 9L and 9L/2B6 tumors were treated with CPA by i.p. injection and killed 15 min later. 4-OH-CPA levels were determined in blood, liver and tumor tissue. Blood levels of 4-OH-CPA were significantly higher than those found in the
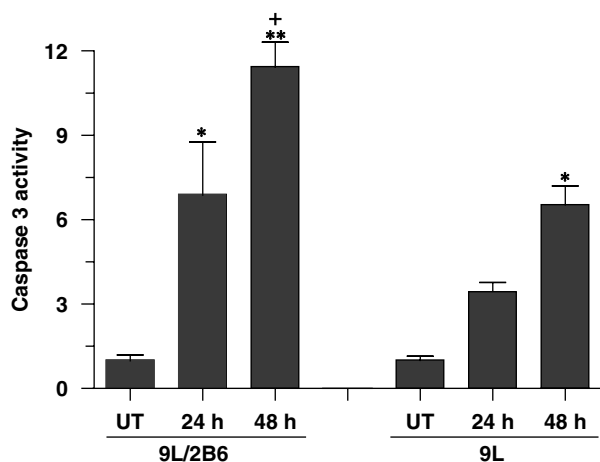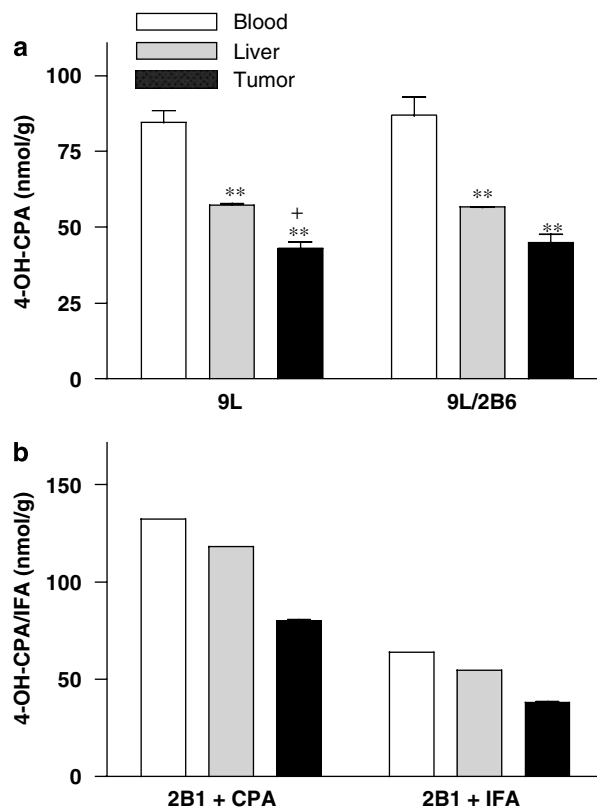
Figure 1 Caspase 3 activity in CPA-treated tumors. Scid mice implanted with 9L or 9L/2B6 tumors were treated with a single i.p. injection of CPA (140 mg kg^{-1} BW) or were untreated. Tumors were collected 24 or 48 h later. Caspase 3 activity was determined in the presence and absence of the caspase 3-selective inhibitor Casputin as described in Materials and methods. Data shown are mean $\pm$ s.e. values ($n = 4$ for CPA-treated tumors; $n = 2$ untreated tumors) relative to UT tumors. Data were analyzed using one-way ANOVA and nonparametric Bonferroni's Multiple Comparison test: $*P < 0.05$ and $**P < 0.01$, respectively, for CPA-treated vs untreated; $^{+}P < 0.05$ for 9L/2B6 vs 9L tumors at the same CPA treatment time. CPA, cyclophosphamide; i.p., intraperitoneal; BW, body weight; UT, untreated; ANOVA, analysis of variance.

Figure 2 Tissue levels of 4-OH-CPA and 4-OH-IFA in mice bearing 9L/2B6, 9L/2B1 and 9L tumors. Scid mice bearing 9L, 9L/2B6 or 9L/2B1 tumors were treated with CPA or IFA, following which tissues were collected and assayed for 4-OH-CPA or 4-OH-IFA by high-performance liquid chromatography. (**a**) Mice bearing 9L or 9L/2B6 tumors were killed 15 min after CPA treatment at 140 mg kg^{-1}. Values shown are mean $\pm$ range for blood and liver ($n = 2$) and mean $\pm$ s.e. for tumors ($n = 4$). Data were analyzed using one-way ANOVA and nonparametric Bonferroni's Multiple Comparison test: $**P < 0.01$ for liver and tumor vs blood; $^{+}P < 0.05$ for tumor vs liver. (**b**) Mice bearing 9L/2B1 tumors were killed 15 min after CPA treatment at 140 mg kg^{-1} or IFA treatment at 300 mg kg^{-1}. Values are shown for blood and liver ($n = 1$) and for tumors (mean $\pm$ range, $n = 2$). CPA, cyclophosphamide; ANOVA, analysis of variance.

liver in both 9L and 9L/2B6 tumors, indicating rapid clearance of this primary metabolite from its site of production in the liver (Figure 2a). Surprisingly, i.t. 4-OH-CPA levels were the same in 9L/2B6 tumors as in 9L tumors, indicating that the major fraction of tumor-associated metabolite is formed extratumorally, that is it is derived from hepatic metabolism. A similar pattern was seen 60 min after drug administration (data not shown). 9L tumors expressing *P*450 2B1, which is a more active CPA 4-hydroxylase than *P*450 2B6,[29] also showed lower 4-OH-CPA levels in tumor compared to blood and liver (Figure 2b). A similar result was obtained in 9L/2B1 tumors treated with IFA, an isomer of CPA that is also activated by 4-hydroxylation (Figure 2b). We conclude that the levels of *P*450 2B6 and *P*450 2B1 expressed in these tumors, while very effective at enhancing CPA's antitumor activity,[24] are too low to measurably increase the 4-hydroxy metabolite above the high background level that results from hepatic *P*450 metabolism.

4-OH-CPA formation in 9L/2B11 tumors
The low K_m of *P*450 2B11 for CPA ($\sim 70 \, \mu$M) translates into superior antitumor activity *in vitro* and in preclinical *P*450 gene therapy models.[24] Given this low K_m, the therapeutic advantage of *P*450 2B11 is expected to be manifest at CPA concentrations that are comparatively low ($\leqslant 100 \, \mu$M), as they are in CPA-treated cancer patients.[30,31] Indeed, although tumor-associated 4-OH-CPA levels were lower in 9L/2B1 and 9L/2B6 tumors than in liver (Figure 2), i.t. 4-OH-CPA concentrations were at

least as high, if not higher than in liver in the case of CPA-treated 9L/2B11 tumors (Figure 3a). Moreover, i.t. 4-OH-CPA concentrations were significantly higher in 9L/2B11 tumors than in 9L tumors over a range of CPA doses (Figure 3b), consistent with the occurrence of substantial i.t. CPA activation. Intratumoral CPA activation also occurs in the case of the high K_m enzymes *P*450 2B6 and *P*450 2B1, as evidenced by the enhanced apoptotic response (Figure 1) and antitumor effect compared to *P*450-deficient tumors,[24] but could not be discerned in the context of the high background level of hepatic *P*450 metabolism. The *P*450 2B11-dependent increase in i.t. 4-OH-CPA was dose-dependent, without reaching saturation at 140 mg CPA kg^{-1} BW (Figure 3c). The inability to saturate the active site of *P*450 2B11 at this dose, which corresponds to a C_{max} (CPA) of $\sim 200 \, \mu$M,[32] suggests there is restricted uptake of circulating CPA by the tumor cells, reducing the availability of CPA for i.t. metabolism.
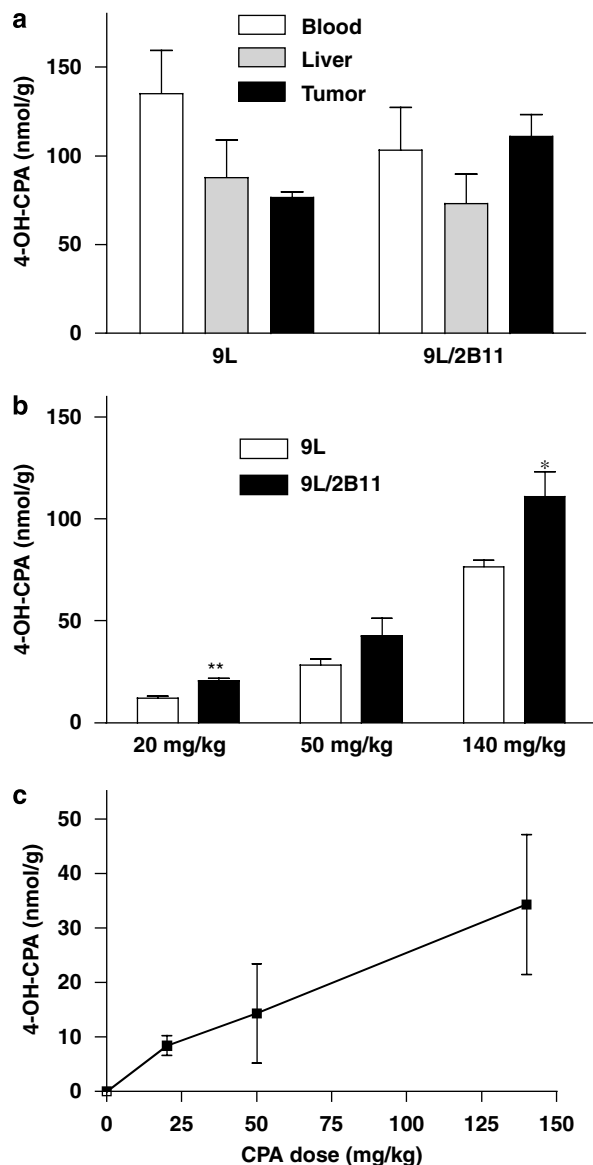
Figure 3 4-OH-CPA levels in mice bearing 9L/2B11 tumors. Scid mice bearing 9L or 9L/2B11 tumors were killed 15 min after i.p. injection of CPA at 20, 50 or 140 mg kg^{-1} BW. (**a**) 4-OH-CPA levels in blood, liver and tumors of mice treated with CPA at 140 mg kg^{-1}. Data shown are mean±range for blood and liver ($n=2$) and mean±s.e. for tumors ($n=4$). (**b**) 4-OH-CPA in 9L and 9L/2B11 tumors from mice treated at the indicated CPA doses. Data shown are mean±s.e. ($n=4$) values. *$P<0.05$ and **$P<0.01$ for 9L/2B11 vs 9L, respectively. (**c**) Increase in tumor-associated 4-OH-CPA in 9L/2B11 tumors compared to 9L tumors as a function of CPA dose. Data shown are mean values±s.e. ($n=4$), calculated by subtracting the mean 4-OH-CPA level in 9L tumors from the mean 4-OH-CPA level in 9L/2B11 tumors at each CPA dose. i.p., intraperitoneal; CPA, cyclophosphamide; BW, body weight.

More detailed pharmacokinetic analyses were carried out to determine how the low K_{m} of *P*450 2B11 impacts the net exposure of tumor and host tissues to activated CPA. In 9L tumors, which do not metabolize CPA, peak concentrations of 4-OH-CPA were detected in blood and liver as early as 6 min after i.p. CPA injection, while tumor 4-OH-CPA levels reached their peak at the 15 min time point (Figure 4a). This difference in T_{max} indicates delayed diffusion of 4-OH-CPA from systemic circulation into the tumor. Moreover, at the 6 min time point, the tumor content of 4-OH-CPA was only 40% of that of blood (17.6 vs 45.4 nmol g^{-1} tissue; Figure 4a). In contrast, in mice bearing 9L/2B11 tumors, 4-OH-CPA concentrations were higher in tumor than in blood or liver at all times after i.p. CPA administration, except at 6 min, where similar levels of 4-OH-CPA, were found in blood and tumor (Figure 4b). Pharmacokinetic analysis revealed that, following i.p. CPA treatment, the C_{max} and area under the curve of drug concentration × time (AUC) of 4-OH-CPA were both significantly higher in 9L/2B11 tumors than in 9L tumors (Table 1). Collectively, these findings provide strong support for the occurrence of substantial i.t. CPA activation catalyzed by the tumor cell-expressed *P*450 2B11.

Impact of intratumoral CPA delivery on 4-OH-CPA pharmacokinetics
The impact of localized, i.t. delivery of CPA on the net exposure of 9L/2B11 tumors, and of host tissue, to 4-OH-CPA was investigated. Intratumoral CPA injection increased the C_{max} and AUC values for tumor exposure to 4-OH-CPA by 1.8- and 2.7-fold, respectively, compared to i.p. CPA treatment (Table 1; 86.2 vs 48.4 nmol g^{-1} tissue for C_{max}; and 60.2 vs 22.4 h · nmol g^{-1} tissue for AUC). Thus, i.t. delivery of CPA increases the availability of CPA for metabolism by the tumor cell-expressed *P*450 2B11. The enhanced i.t. metabolism of CPA was accompanied by a significant decrease in C_{max} of 4-OH-CPA in both blood and liver, consistent with a shift in CPA metabolism from the liver to the tumor (Figure 4c vs Figure 4b; Table 1). However, no significant change in the AUC of 4-OH-CPA was observed in either blood or liver when i.t. CPA and i.p. CPA were compared.

Next, we investigated whether further increases in i.t. CPA 4-hydroxylation could be achieved using the slow release polymer F127 to increase the residence time of CPA in the tumor, and thereby increase the likelihood that the prodrug will be metabolized by the tumor cell-expressed *P*450, that is, before it diffuses out from the tumor and into systemic circulation. F127 is soluble at 4 °C but increases in viscosity and forms a gel when the temperature is raised to 37 °C, as occurs following i.t. injection.[33] Intratumoral delivery of CPA using a 23% solution of F127 significantly increased the AUC of tumor-associated 4-OH-CPA when compared to i.t. injection without polymer, and significantly decreased the C_{max} of 4-OH-CPA in both blood and liver (Figure 4d vs Figure 4c; Table 1). The lower C_{max} in blood suggests that there is reduced exposure of other organs to activated CPA. Both the $t_{1/2}$ and the AUC of 4-OH-CPA in liver were increased by i.t. injection of CPA with polymer as compared to i.t. CPA injection without polymer or to i.p. CPA injection (Table 1). These findings suggest that the slow release of CPA from its i.t. delivery site decreases
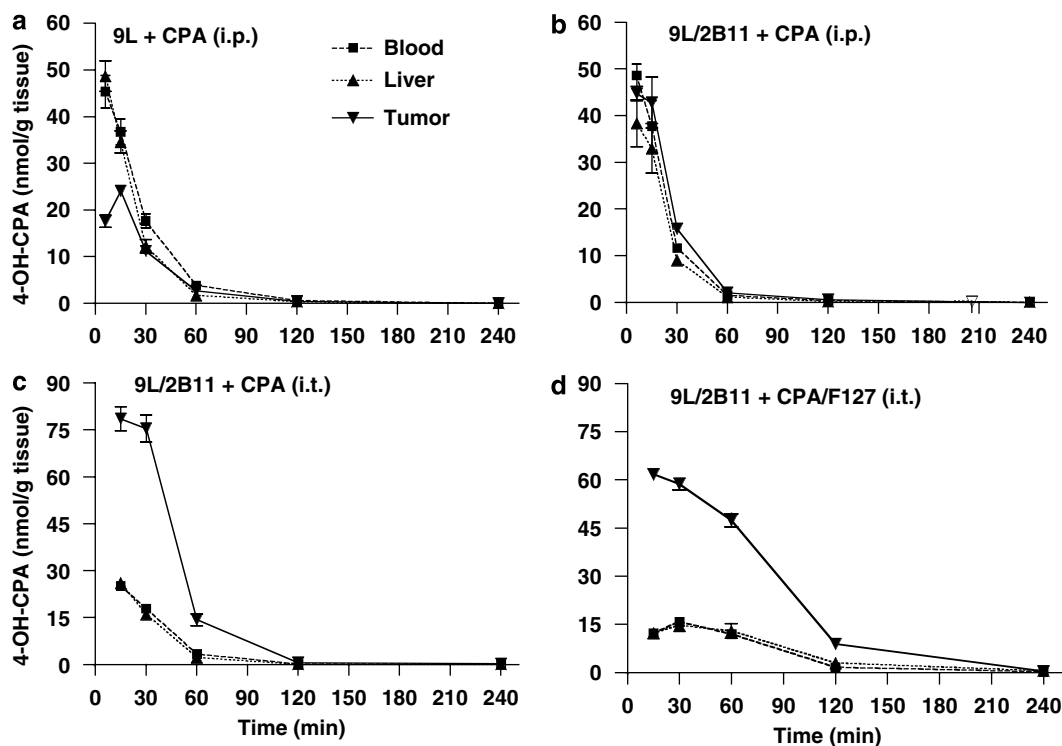
Figure 4 Effect of i.t. CPA delivery on pharmacokinetics of 4-OH-CPA in mice bearing 9L/2B11 tumors. Scid mice bearing 9L (**a**) or 9L/2B11 tumors (**b–d**) were killed 6–240 min after treatment with CPA by i.p. (**a** and **b**) or i.t. (**c** and **d**) injection at 50 mg kg^{-1} BW. Cyclophosphamide was dissolved in 0.2% NaCl (**a–c**) or in 23% F127/NaCl (**d**). Data shown are 4-OH-CPA levels (mean $\pm$ s.e.; $n = 3$ for blood and liver, $n = 6$ for tumors). Tissue collection and 4-OH-CPA analysis were as described in Materials and methods. i.t., intratumoral; CPA, cyclophosphamide; i.p., intraperitoneal; BW, body weight.

Table 1 Pharmacokinetics of 4-OH-CPA in mice bearing 9L/2B11 or 9L tumors

Tissue	Parameter	9L, i.p. CPA	9L/2B11, i.p. CPA	9L/2B11, i.t. CPA	9L/2B11, i.t. CPA $\pm$ F127
Blood	C_{max} (nmol g^{-1})	45.4$\pm$3.7	50.2$\pm$1.6	22.6$\pm$1.4[a]	15.6$\pm$0.5[b,c]
	$t_{1/2}$ (min)	18.0$\pm$0.3	15.4$\pm$1.0	33.6$\pm$2.1[a]	32.8$\pm$4.4[d]
	AUC$_{INF}$ (h$\cdot$nmol g^{-1})	23.3$\pm$0.8	20.1$\pm$0.9	16.0$\pm$2.7	21.1$\pm$1.2
Liver	C_{max} (nmol g^{-1})	48.8$\pm$3.2	44.6$\pm$2.4	23.6$\pm$1.9[a]	16.3$\pm$1.4[b,e]
	$t_{1/2}$ (min)	15.9$\pm$0.3	23.8$\pm$0.6[f]	23.9$\pm$6.2	41.8$\pm$2.0[b]
	AUC$_{INF}$ (h$\cdot$nmol g^{-1})	19.1$\pm$1.1	16.3$\pm$0.5	14.3$\pm$2.9	23.8$\pm$1.2[b,e]
Tumor	C_{max} (nmol g^{-1})	24.1$\pm$0.5	48.4$\pm$3.4[f]	86.2$\pm$11.4[g]	64.9$\pm$2.9[b]
	$t_{1/2}$ (min)	20.0$\pm$0.1	19.5$\pm$1.5	27.0$\pm$1.5[a]	29.8$\pm$1.0[b]
	AUC$_{INF}$ (h$\cdot$nmol g^{-1})	13.7$\pm$0.7	22.4$\pm$1.1[f]	60.2$\pm$7.6[a]	87.2$\pm$4.3[b,e]

Abbreviations: AUC, area under the curve of drug concentration $\times$ time; C_{max}, maximum concentration; CPA, cyclophosphamide; F127, Pluronic F127 block copolymer; i.p., intraperitoneal; i.t., intratumoral.
Data shown are mean values $\pm$ s.e., with each data point determined for $n = 3$ mice.
[a]$P < 0.01$ for 9L/2B11 tumors treated with i.p. CPA vs i.t. CPA.
[b]$P < 0.01$ for 9L/2B11 tumors treated with i.t. CPA/F127 vs i.p. CPA.
[c]$P < 0.01$ for 9L/2B11 tumors treated with i.t. CPA/F127 vs i.t. CPA without F127.
[d]$P < 0.05$ for 9L/2B11 tumors treated with i.t. CPA/F127 vs i.p. CPA.
[e]$P < 0.05$ for 9L/2B11 tumors treated with i.t. CPA/F127 vs i.t. CPA without F127.
[f]$P < 0.01$ for i.p. CPA treatment of 9L/2B11 vs 9L tumors.
[g]$P < 0.05$ for 9L/2B11 tumors treated with i.p. CPA vs i.t. CPA.

hepatic CPA levels, which in turn leads to metabolism of CPA over an extended period of time.

Impact of intratumoral, slow release CPA delivery on antitumor activity

We investigated the impact on antitumor activity of the increased exposure of 9L/2B11 tumors to 4-OH-CPA achieved by using F127 for i.t. CPA delivery. Scid mice bearing 9L/2B11 tumors were treated with CPA using a maximally tolerated dose schedule (2×150 mg CPA kg^{-1} BW). Cyclophosphamide was administered by i.p. injection or by i.t. injection using F127 as the vehicle. 9L/2B11 tumor growth was halted immediately in both CPA treatment groups (Figure 5a). However, the mice treated with i.t. CPA/F127 showed significant tumor regression beginning on day 11, whereas tumor regression was not observed in the mice treated with i.p. CPA until day 21 after CPA treatment. Moreover, the maximal tumor regression was significantly higher in the i.t. CPA/ F127 treatment group (87 vs 53% regression; $P < 0.0005$). A second cycle of CPA treatment at day 35 effected substantial tumor growth delay but not tumor regression in either group, perhaps reflecting a preferential killing of *P450* 2B11-expressing tumor cells in the first treatment cycle and indicating a need for multiple rounds of *P450* gene delivery *in vivo* for effective implementation of this strategy in the clinic. Cyclophosphamide-induced BW loss was more pronounced in the mice receiving CPA via the F127 vehicle, suggesting some intrinsic toxicity of this polymer (Figure 5b).

Discussion

The efficacy of *P450*-based gene therapy, like that of other prodrug activation strategies, depends on three key factors: (1) the effectiveness of gene delivery *in vivo*; (2) the catalytic efficiency of the prodrug activation system; and (3) the biochemical and physicochemical factors that govern the metabolism, pharmacokinetics and cellular responses to the prodrug and its activated metabolites. Recent advances in vector technology have facilitated tumor-selective delivery of prodrug-activation genes and their controlled propagation as regulated by tumor-specific genetic factors and the tumor's physiological state.[34–36] Significant technical limitations in gene transfer efficiency remain, however, but can in part be compensated for by mutations that increase the catalytic activity or efficiency of the prodrug activation gene.[37–39] In the case of cytochrome *P450*, the low catalytic efficiency of the high K_m CPA 4-hydroxylase enzymes *P450* 2B1 and *P450* 2B6 toward the anticancer prodrug substrate CPA ($K_m \sim 500$–1500 μM) can be greatly improved by the use of *P450* 2B11, a low K_m CPA 4-hydroxylase ($K_m \sim 70$ μM).[24] Presently, we used scid mice bearing 9L gliosarcomas transduced with retrovirus encoding either high K_m or low K_m CPA-activating *P450* enzymes as a model system to characterize the metabolic and pharmacokinetic factors that underlie this improved activity and to investigate the impact of i.t. CPA delivery using a slow release polymer.

Tissue concentrations of 4-OH-CPA, the primary activated metabolite of CPA, were lower in tumor than in blood and liver following CPA treatment of mice bearing 9L/2B6 and 9L/2B1 tumors. Moreover, i.t. 4-OH-CPA levels in 9L/2B6 and 9L/2B1 tumors were indistinguishable from those in *P450*-deficient 9L tumors. A similar observation was made in the case of human glioma xenografts infected with Herpes virus encoding *P450* 2B1.[40] Thus, in mice with tumors expressing *P450* 2B6 or *P450* 2B1, the vast majority of tumor-associated 4-OH-CPA is still derived from the liver, which is much larger in size and has a higher content of cytochrome *P450* than the *P450*-expressing tumors. Nevertheless, 9L/ 2B6 and 9L/2B1 tumors both display enhanced CPA chemosensitivity[13,28] and enhanced apoptotic responses compared to control 9L tumors, as was shown for
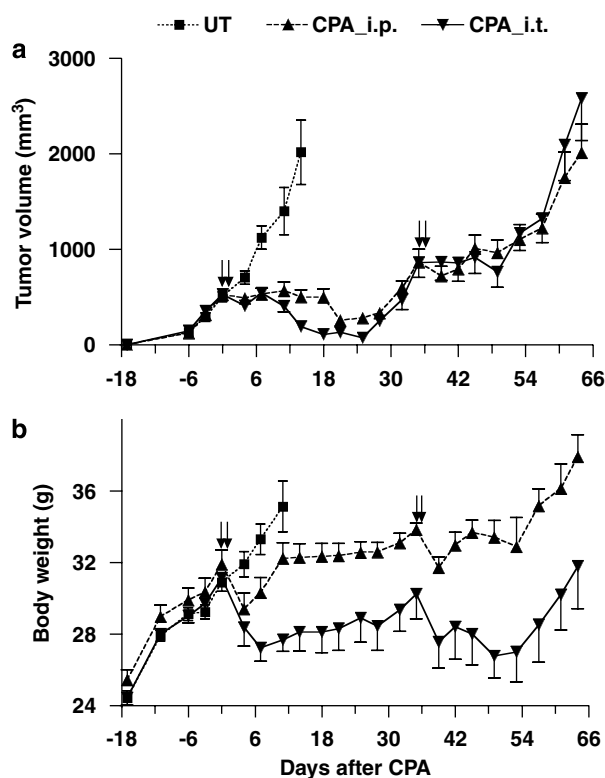
Figure 5 Effect of i.t. CPA delivery on growth of 9L/2B11 tumors. 9L/2B11 tumors were implanted s.c. and grown in male scid mice. Tumor volumes (**a**) and BW (**b**) were measured twice a week. X axis, days prior to (negative values) or after first CPA injection. Pair of arrows indicate maximally tolerated dose CPA administration schedule: two CPA injections, each at 150 mg kg^{-1} and spaced 24 h apart. Solid square, untreated group; solid triangle, CPA injection i.p. without polymer; inverted solid triangle, i.t. CPA delivery with 23% F127. Tumor data shown are mean ± s.e. values ($n = 10$). Tumor doubling time was 6.4 ± 0.7 days for untreated tumors vs > 36 days for the CPA-treated tumors. Tumors treated with CPA/23% F127 regressed more rapidly, and more completely than following i.p. CPA treatment. i.t., intratumoral; CPA, cyclophosphamide; s.c., subcutaneously; BW, body weight.

CPA-treated 9L/2B6 tumors (caspase 3 activity; Figure 1). This suggests that while liver-derived 4-OH-CPA may readily enter blood vessels associated with 9L tumors, it has only limited access to the relevant tumor cell compartments. As a consequence, liver-derived 4-OH-CPA is apparently much less effective at inducing tumor cell apoptosis and an overall antitumor response when compared to a much lower level of 4-OH-CPA formed directly within tumor cells via i.t. P450 metabolism. Of note, 4-OH-CPA undergoes chemical decomposition to release phosphoramide mustard, a DNA crosslinking agent and the ultimate therapeutic metabolite, which unlike 4-OH-CPA, has restricted cell membrane permeability.[41] Accordingly, any 4-OH-CPA molecules that decompose to phosphoramide mustard within tumor-associated blood vessels, or within the initial layers of tumor cells adjacent to the tumor vasculature, are unlikely to induce widespread tumor cell cytotoxic responses. Circulating 4-OH-CPA itself also appears to have restricted access to 9L tumors, as indicated by the 4-OH-CPA levels being consistently lower in the 9L tumors than in blood or liver, despite the fact that 9L tumors are well vascularized.[42]

In contrast to 9L/2B6 and 9L/2B1 tumors, whose catalysis of 4-OH-CPA formation was undetectable in the context of the high background of liver-derived 4-OH-CPA, i.t. formation of 4-OH-CPA by 9L/2B11 tumors was readily evident following systemic CPA administration and was associated with 4-OH-CPA levels significantly higher than in blood and liver. The high level of i.t. CPA activation thus achieved in 9L/2B11 tumors is likely to be key to the substantially improved CPA antitumor response displayed in gene therapy models using P450 2B11 as compared to P450 2B6 or P450 2B1.[24] Together, these findings provide proof-of-principle for the use of low K_m prodrug-activation enzymes, such as P450 2B11 and improved variants,[43] to augment i.t. prodrug activation at pharmacologically relevant prodrug dosages. These findings will need to be verified using viral or other gene therapy vectors to deliver P450 genes to solid tumors in vivo, where P450 protein expression is likely to be much realized in a much smaller fraction of tumor cells than the up to 50% tumor cell coverage seen here.

Physiological conditions associated with solid tumors often lead to poor drug uptake,[44,45] which in the case of prodrug activation gene therapy may translate into inefficient prodrug activation. Presently, 4-OH-CPA production by P450 2B11-expressing 9L tumors was not saturated at a prodrug dose corresponding to a C_{max} (CPA) of $\sim 200\,\mu M$, that is ~ 3 times the observed K_m of P450 2B11, suggesting inefficient penetration of CPA, despite the good vascularity of 9L tumors. To circumvent this problem, CPA was administered by direct i.t. injection, which significantly improved i.t. 4-OH-CPA pharmacokinetics, as evidenced by a 1.8-fold increase in C_{max} and a 2.7-fold increase in AUC compared to systemic CPA treatment. Further improvements were obtained using the slow release polymer poloxamer 407 (F127) as vehicle for CPA delivery. This biocompatible polymer dissolves in aqueous solution at 4 °C, but rapidly

forms a gel upon shifting the temperature to 37 °C and can be used to effect slow release of lipophilic drugs and other small molecules as well as large particles such as viruses.[23,33,46] Overall exposure of the tumor mass to 4-OH-CPA was increased 3.9-fold by i.t. CPA delivery via the slow release polymer, as indicated by AUC, and antitumor activity was correspondingly enhanced, as indicated by early onset and more extensive tumor regression. The effective increase in tumor cell exposure to 4-OH-CPA is likely to be even greater than the measured 3.9-fold increase in AUC, given that a substantial fraction of the AUC (4-OH-CPA) under conditions of i.p. CPA treatment is liver-derived 4-OH-CPA, which as discussed above, has poor access to the relevant tumor cell compartment. Peak host tissue 4-OH-CPA levels were also reduced with i.t. CPA delivery, both with and without the slow release polymer, and this may translate into a reduction of toxicity to sensitive host tissues. Localized chemotherapy may thus be used to shift the partitioning of P450 prodrug from the liver to the tumor. This general strategy may be implemented in a variety of ways, including using other slow release polymers that may be better optimized for small hydrophilic drugs such as CPA[40] or may be more suitable for clinical studies, or by localized instillation of prodrug to the tumor vasculature, as exemplified by preclinical and clinical studies of P450 prodrug gene therapy in pancreatic cancer.[21,47]

Abbreviations

AUC, area under the curve of drug concentration × time; BW, body weight; C_{max}, maximum concentration; CPA, cyclophosphamide; DMEM, Delbecco's modified Eagle's medium; F127, Pluronic F127 or poloxamer 407 block copolymer; FBS, fetal bovine serum; IFA, ifosfamide.

Acknowledgements

References

1 McKeown SR, Ward C, Robson T. Gene-directed enzyme prodrug therapy: a current assessment. *Curr Opin Mol Ther* 2004; **6**: 421–435.

2 Shinohara ET, Lu B, Hallahan DE. The use of gene therapy in cancer research and treatment. *Technol Cancer Res Treat* 2004; **3**: 479–490.

3 Dachs GU, Tupper J, Tozer GM. From bench to bedside for gene-directed enzyme prodrug therapy of cancer. *Anticancer Drugs* 2005; **16**: 349–359.

4 Roy P, Waxman DJ. Activation of oxazaphosphorines by cytochrome P450: application to gene-directed enzyme prodrug therapy for cancer. *Toxicol In Vitro* 2006; **20**: 176–186.

5 Jounaidi Y. Cytochrome *P450*-based gene therapy for cancer treatment: from concept to the clinic. *Curr Drug Metab* 2002; **3**: 609–622.

6 Huang Z, Fasco MJ, Figge HL, Keyomarsi K, Kaminsky LS. Expression of cytochromes *P450* in human breast tissue and tumors. *Drug Metab Dispos* 1996; **24**: 899–905.

7 Murray GI, McFadyen MC, Mitchell RT, Cheung YL, Kerr AC, Melvin WT. Cytochrome *P450* CYP3A in human renal cell cancer. *Br J Cancer* 1999; **79**: 1836–1842.

8 Scripture CD, Sparreboom A, Figg WD. Modulation of cytochrome *P450* activity: implications for cancer therapy. *Lancet Oncol* 2005; **6**: 780–789.

9 McFadyen MC, Melvin WT, Murray GI. Cytochrome *P450* enzymes: novel options for cancer therapeutics. *Mol Cancer Ther* 2004; **3**: 363–371.

10 Chen L, Waxman DJ. Cytochrome *P450* gene-directed enzyme prodrug therapy (GDEPT) for cancer. *Curr Pharm Des* 2002; **8**: 1405–1416.

11 Hudis CA, Schmitz N. Dose-dense chemotherapy in breast cancer and lymphoma. *Semin Oncol* 2004; **31**: 19–26.

12 Roy P, Yu LJ, Crespi CL, Waxman DJ. Development of a substrate-activity based approach to identify the major human liver P-450 catalysts of cyclophosphamide and ifosfamide activation based on cDNA-expressed activities and liver microsomal P-450 profiles. *Drug Metab Dispos* 1999; **27**: 655–666.

13 Chen L, Waxman DJ. Intratumoral activation and enhanced chemotherapeutic effect of oxazaphosphorines following cytochrome *P450* gene transfer: development of a combined chemotherapy/cancer gene therapy strategy. *Cancer Res* 1995; **55**: 581–589.

14 Jounaidi Y, Waxman DJ. Combination of the bioreductive drug tirapazamine with the chemotherapeutic prodrug cyclophosphamide for *P450*/*P450*-reductase-based cancer gene therapy. *Cancer Res* 2000; **60**: 3761–3769.

15 McCarthy HO, Yakkundi A, McErlane V, Hughes CM, Keilty G, Murray M *et al*. Bioreductive GDEPT using cytochrome *P450* 3A4 in combination with AQ4N. *Cancer Gene Ther* 2003; **10**: 40–48.

16 Browder T, Butterfield CE, Kraling BM, Shi B, Marshall B, O'Reilly MS *et al*. Antiangiogenic scheduling of chemotherapy improves efficacy against experimental drug-resistant cancer. *Cancer Res* 2000; **60**: 1878–1886.

17 Jounaidi Y, Waxman DJ. Frequent, moderate-dose cyclophosphamide administration improves the efficacy of cytochrome P-450/cytochrome P-450 reductase-based cancer gene therapy. *Cancer Res* 2001; **61**: 4437–4444.

18 Tyminski E, Leroy S, Terada K, Finkelstein DM, Hyatt JL, Danks MK *et al*. Brain tumor oncolysis with replication-conditional herpes simplex virus type 1 expressing the prodrug-activating genes, CYP2B1 and secreted human intestinal carboxylesterase, in combination with cyclophosphamide and irinotecan. *Cancer Res* 2005; **65**: 6850–6857.

19 Jounaidi Y, Waxman DJ. Use of replication-conditional adenovirus as a helper system to enhance delivery of *P450* prodrug-activation genes for cancer therapy. *Cancer Res* 2004; **64**: 292–303.

20 Braybrooke JP, Slade A, Deplanque G, Harrop R, Madhusudan S, Forster MD *et al*. Phase I study of MetXia-*P450* gene therapy and oral cyclophosphamide for patients with advanced breast cancer or melanoma. *Clin Cancer Res* 2005; **11**: 1512–1520.

21 Salmons B, Lohr M, Gunzburg WH. Treatment of inoperable pancreatic carcinoma using a cell-based local chemotherapy: results of a phase I/II clinical trial. *J Gastroenterol* 2003; **38** (Suppl 15): 78–84.

22 Chen CS, Lin JT, Goss KA, He YA, Halpert JR, Waxman DJ. Activation of the anticancer prodrugs cyclophosphamide and ifosfamide: identification of cytochrome *P450* 2B enzymes and site-specific mutants with improved enzyme kinetics. *Mol Pharmacol* 2004; **65**: 1278–1285.

23 Kabanov A, Zhu J, Alakhov V. Pluronic block copolymers for gene delivery. *Adv Genet* 2005; **53PA**: 231–261.

24 Jounaidi Y, Chen CS, Veal GJ, Waxman DJ. Enhanced antitumor activity of *P450* prodrug-based gene therapy using the low Km cyclophosphamide 4-hydroxylase *P450* 2B11. *Mol Cancer Ther* 2006; **5**: 541–555.

25 Schwartz PS, Waxman DJ. Cyclophosphamide induces caspase 9-dependent apoptosis in 9L tumor cells. *Mol Pharmacol* 2001; **60**: 1268–1279.

26 Wagner KD, Wagner N, Wellmann S, Schley G, Bondke A, Theres H *et al*. Oxygen-regulated expression of the Wilms' tumor suppressor Wt1 involves hypoxia-inducible factor-1 (HIF-1). *FASEB J* 2003; **17**: 1364–1366.

27 Huang Z, Raychowdhury MK, Waxman DJ. Impact of liver *P450* reductase suppression on cyclophosphamide activation, pharmacokinetics and antitumoral activity in a cytochrome *P450*-based cancer gene therapy model. *Cancer Gene Ther* 2000; **7**: 1034–1042.

28 Jounaidi Y, Hecht JE, Waxman DJ. Retroviral transfer of human cytochrome *P450* genes for oxazaphosphorine-based cancer gene therapy. *Cancer Res* 1998; **58**: 4391–4401.

29 Chen CS, Jounaidi Y, Waxman DJ. Enantioselective metabolism and cytotoxicity of R-ifosfamide and S-ifosfamide by tumor cell-expressed cytochromes *P450*. *Drug Metab Dispos* 2005; **33**: 1261–1267.

30 Busse D, Busch FW, Bohnenstengel F, Eichelbaum M, Fischer P, Opalinska J *et al*. Dose escalation of cyclophosphamide in patients with breast cancer: consequences for pharmacokinetics and metabolism. *J Clin Oncol* 1997; **15**: 1885–1896.

31 Chan KK, Hong PS, Tutsch K, Trump DL. Clinical pharmacokinetics of cyclophosphamide and metabolites with and without SR-2508. *Cancer Res* 1994; **54**: 6421–6429.

32 Gu J, Chen CS, Wei Y, Fang C, Xie F, Kannan K *et al*. A mouse model with liver-specific deletion and global suppression of the NADPH-cytochrome *P450* reductase gene: characterization and utility for *in vivo* studies of cyclophosphamide disposition. *J Pharmacol Exp Ther* 2007; **321**: 9–17.

33 Wang Y, Liu S, Li CY, Yuan F. A novel method for viral gene delivery in solid tumors. *Cancer Res* 2005; **65**: 7541–7545.

34 Saukkonen K, Hemminki A. Tissue-specific promoters for cancer gene therapy. *Expert Opin Biol Ther* 2004; **4**: 683–696.

35 Brown JM, Wilson WR. Exploiting tumour hypoxia in cancer treatment. *Nat Rev Cancer* 2004; **4**: 437–447.

36 McCormick F. Cancer-specific viruses and the development of ONYX-015. *Cancer Biol Ther* 2003; **2**(Suppl 1): S157–S160.

37 Kokoris MS, Sabo P, Adman ET, Black ME. Enhancement of tumor ablation by a selected HSV-1 thymidine kinase mutant. *Gene Ther* 1999; **6**: 1415–1426.

38 Kievit E, Bershad E, Ng E, Sethna P, Dev I, Lawrence TS *et al*. Superiority of yeast over bacterial cytosine deaminase for enzyme/prodrug gene therapy in colon cancer xenografts. *Cancer Res* 1999; **59**: 1417–1421.

39 Bennett EM, Anand R, Allan PW, Hassan AE, Hong JS, Levasseur DN *et al*. Designer gene therapy using an *Escherichia coli* purine nucleoside phosphorylase/prodrug system. *Chem Biol* 2003; **10**: 1173–1181.

10

40 Ichikawa T, Petros WP, Ludeman SM, Fangmeier J, Hochberg FH, Colvin OM *et al*. Intraneoplastic polymer-based delivery of cyclophosphamide for intratumoral bio-conversion by a replicating oncolytic viral vector. *Cancer Res* 2001; **61**: 864–868.

41 Sladek NE. Metabolism of oxazaphosphorines. *Pharmacol Ther* 1988; **37**: 301–355.

42 Kirsch M, Strasser J, Allende R, Bello L, Zhang J, Black PM. Angiostatin suppresses malignant glioma growth *in vivo*. *Cancer Res* 1998; **58**: 4654–4659.

43 Sun L, Chen CS, Waxman DJ, Liu H, Halpert JR, Kumar S. Re-engineering cytochrome *P*450 2B11dH for enhanced metabolism of several substrates including the anti-cancer prodrugs cyclophosphamide and ifosfamide. *Arch Biochem Biophys* 2007; **458**: 167–174.

44 Cairns R, Papandreou I, Denko N. Overcoming physiologic barriers to cancer treatment by molecularly targeting the tumor microenvironment. *Mol Cancer Res* 2006; **4**: 61–70.

45 Reddy LH. Drug delivery to tumours: recent strategies. *J Pharm Pharmacol* 2005; **57**: 1231–1242.

46 Dumortier G, Grossiord JL, Agnely F, Chaumeil JC. A review of poloxamer 407 pharmaceutical and pharmacological characteristics. *Pharm Res* 2006; **23**: 2709–2728.

47 Lohr M, Hoffmeyer A, Kroger J, Freund M, Hain J, Holle A *et al*. Microencapsulated cell-mediated treatment of inoperable pancreatic carcinoma. *Lancet* 2001; **357**: 1591–1592.